Aquaculture 615 (2026) 743593

Contents lists available at ScienceDirect

Aquaculture

journal homepage: www.elsevier.com/locate/aquaculture

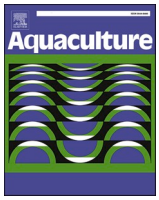

Impaired Sertoli-Spermatogonia interactions contribute to oligospermia and infertility in F1 captive-bred male *Solea senegalensis*

Guillermo Barturen [a,b,c,*], Diego Robledo [d], Francisca Robles [a], Rose Ruiz Daniels [e], Maialen Carballeda [f], Dorinda Torres-Sabino [f], Rafael Navajas-Pérez [a], Paulino Martínez [f], Carmelo Ruiz-Rejón [a], Roberto De la Herrán [a,*]

[a] Department of Genetics, Faculty of Science, University of Granada, 18071 Granada, Spain
[b] Bioinformatics Laboratory, Biotechnology Institute, Centro de Investigación Biomédica, PTS, Avda. del Conocimiento s/n, 18100 Granada, Spain
[c] Genyo, Pfizer–University of Granada–Junta de Andalucía Centre for Genomics and Oncological Research, Granada, Spain
[d] Department of Zoology, Genetics and Physical Anthropology, Universidade de Santiago de Compostela, Faculty of Biology, 15782 Santiago de Compostela, Spain
[e] Institute of Aquaculture, University of Stirling, Stirling, UK
[f] Department of Zoology, Genetics and Physical Anthropology, Universidade de Santiago de Compostela, Faculty of Veterinary, 27002 Lugo, Spain

ARTICLE INFO

Keywords:
Solea senegalensis
snRNA-Seq
Infertility
Captive-bred
Gonad

ABSTRACT

Reproductive dysfunction of captive-bred males of the Senegalese sole (*Solea senegalensis*) represents a significant bottleneck for its aquaculture, as these fish exhibit reduced sperm production and impaired fertility compared to wild-bred counterparts acclimated to farm conditions. To elucidate the cellular and molecular mechanisms underlying this phenomenon, single-nuclei RNA sequencing was performed on gonadal tissue from adult captive-bred and wild-bred males. The analysis yielded a high-quality dataset comprising ~80.000 cells, which were grouped into eleven distinct clusters representing all major germline and somatic cell types, including spermatogonial stem cells, differentiating spermatogonia, spermatocytes, spermatids, Sertoli cells, Leydig cells, immune cells, and peritubular myoid cells. It is noteworthy that captive-bred males exhibited a marked overrepresentation of proliferative spermatogonia and a significant reduction in mature spermatids, suggesting a disruption in the progression of spermatogenesis. Differential expression and functional enrichment analyses revealed that spermatogonial cells in captive-bred males displayed heightened translational activity alongside downregulation of pathways related to cell-cell communication and interaction. Focused *in-silico* cell-cell communication analyses further suggested potential defective Sertoli-spermatogonia interactions as a key factor contributing to oligospermia and infertility of captive-bred males. This study provides the first single-nuclei transcriptomic atlas of the Senegalese sole male gonad, offering valuable insights into the molecular basis of reproductive failure in captivity related to gonadal development. The findings of the study will inform future strategies to enhance selective breeding and improve aquaculture productivity for this economically important species.

1. Introduction

Adaptation to the captive aquaculture environment entails complex changes in animal behavior, physiology, and welfare, requiring species-specific strategies to ensure optimal acclimation (Duarte et al., 2007; Zhang et al., 2023). Key challenges in aquaculture production include nutrition, disease management, and, critically, reproductive success (FAO, 2022). Therefore, establishing an efficient captive breeding system is a fundamental prerequisite for sustainable production. This requires not only the optimization of management protocols, such as spawning, incubation and hatchery practices, but also consideration of both intentional and unintentional selection pressures associated with domestication (Bélteky et al., 2018; Gjedrem and Baranski, 2009). Nevertheless, reproductive dysfunctions are frequently observed in

* Corresponding authors at: Department of Genetics, Faculty of Science, University of Granada, 18071 Granada, Spain.
E-mail addresses: gbarturen@ugr.es (G. Barturen), diego.robledo.sanchez@usc.es (D. Robledo), frobles@ugr.es (F. Robles), rose.ruizdaniels@stir.ac.uk (R. Ruiz Daniels), maialen.carballeda@rai.usc.es (M. Carballeda), dorinda.torres@rai.usc.es (D. Torres-Sabino), rnavajas@ugr.es (R. Navajas-Pérez), paulino.martinez@usc.es (P. Martínez), carmelo@ugr.es (C. Ruiz-Rejón), rherran@ugr.es (R. De la Herrán).

https://doi.org/10.1016/j.aquaculture.2025.743593
Received 7 August 2025; Received in revised form 29 November 2025; Accepted 24 December 2025
Available online 25 December 2025

captive fish populations, including delayed or incomplete gametogenesis, reduced levels of sex hormones, smaller and lighter eggs, and diminished reproductive success, often associated to abnormal behaviors (Milla et al., 2021). Effective breeding programs, which are essential in the competitive aquaculture industry, can only be implemented once these reproductive challenges are successfully addressed (De Silva et al., 2008).

Flatfish aquaculture includes several commercial valuable species, such as turbot (*Scophthalmus maximus*), Japanese flounder (*Paralichthys olivaceus*), and tongue sole (*Cynoglossus semilaevis*), for which selective breeding programs supported by standardized reproductive protocols have been successfully established (Munroe, 2021; Robledo et al., 2017). Among European aquaculture candidates, the Senegalese sole (*Solea senegalensis*) stands out as one of the most promising species due to its excellent flesh quality and high market value (Morais et al., 2016). However, reproduction remains a major challenge, as captive-bred males exhibit reproductive dysfunction, most notably the failure to perform courtship behavior. In addition, males that have been born and raised in captivity, captive-bred animals or usually called F1 (CB) (Riesco et al., 2019), have been reported to produce low and variable sperm volumes (Beirão et al., 2011; Cabrita et al., 2006; Ramos-Júdez et al., 2021), significantly lower than their wild counterparts (Cabrita et al., 2006). In particular, Cabrita et al. demonstrated that CB males produced sperm volumes ranging from 5 to 38 μL, with concentrations of 0.7–1.2 $\times 10^9$ spermatozoa/mL and total sperm production below 20 $\times 10^6$ spermatozoa per stripping, whereas WB males reached 10 to 58 μL, 1–2 $\times 10^9$ spermatozoa/mL, and 40–60 $\times 10^6$ spermatozoa per stripping during peak spermiation. Although motility was generally high in both groups (~80 % during peak periods), CB males exhibited shorter and less consistent spermiation cycles (Cabrita et al., 2006). These phenotypic differences hamper the use of in vitro fertilization techniques and limit the implementation of efficient selective breeding programs. In contrast, wild-bred (WB) males acclimated to captive conditions can reproduce successfully (Martín et al., 2019; Riesco et al., 2019). Notably, this reproductive dysfunction is not observed in CB females, which are able to reproduce with WB males (Martín et al., 2019). This sex-specific impairment in CB males presents a significant challenge to the sustainability and competitiveness of the Senegalese sole aquaculture industry.

To investigate the causes of reproductive failure in CB Senegalese sole males, various approaches have been undertaken, including studies on molecular clocks involved in feeding, photoperiod regulation, and reproduction (Gilannejad et al., 2021; López-Olmeda et al., 2016; Martín-Robles et al., 2012), as well as investigations into the endocrine mechanisms controlling gonadal development and maturation (Aliaga-Guerrero et al., 2018; Chauvigné et al., 2016; Oliveira et al., 2020). However, the molecular mechanism underlying the abnormal gonadal maturation and reproduction failure in CB males remain poorly understood. Currently, genomic resources for the Senegalese sole are now well developed, including a highly contiguous, chromosome-level genome assembly with comprehensive annotation, providing a solid foundation for investigating the genetic and regulatory factors underlying reproduction (Benzekri et al., 2014; De la Herrán et al., 2023; Guerrero-Cózar et al., 2021). In addition, recent advances in high-throughput genomics, particularly single-nuclei transcriptomics, offer powerful tools to unravel the cellular and molecular basis of these dysfunctions by enabling detailed characterization of gonadal differentiation and gene expression at single-nuclei resolution.

In this study, we conducted a single-nuclei RNA sequencing (snRNA-Seq) of the gonads from adult *S. senegalensis* males, comparing two CB and two WB individuals. Sexually mature fish were chosen to enable a direct comparison of gonadal cell composition and gene expression profiles between WB males, capable of successful reproduction in captivity, and CB males, which exhibit reduced reproductive performance. To our knowledge, this represents the first single-nucleil transcriptomic analysis of the male gonad in *S. senegalensis*. This study lays the groundwork for future research aimed at resolving reproductive dysfunction and enhancing the aquaculture production of this species, highlighting the potential of single-nuclei genomics to inform targeted interventions and improve selective breeding outcomes.

2. Results

2.1. Single-nuclei RNA-Seq analysis of S. senegalensis gonads yielded a good number of high-quality cells

Single-nuclei RNA-Seq analysis using the 10× Genomics protocol was performed on gonads from two CB and two WB acclimated to farm conditions *S. senegalensis* males. After background removal with Cell Ranger (Zheng et al., 2017) and filtering out cells with fewer than 500 reads, 46,757 and 38,749 cells from CB and WB animals, respectively, were included in the analysis. Additionally, 3476 genes with more than 3 reads in at least 50 cells were selected for further analyses.

Only a few cells showed an elevated percentage of mitochondrial RNA, which indicates a low percentage of dying cells (Supplementary Fig. 1 A). After filtering out cells with mitochondrial RNA content above 10 % and ribosomal RNA content below 1 %, few cells were removed, barely noticeable in the quality control plots after removing these low-quality cells (Supplementary Fig. 1B). For three of the samples (CB2, WB1 and WB2) sequencing saturation in terms of number of unique genes per sequenced molecules was reached, and most of the cells aligned to the best fit line showing a good relationship between sequenced depth and number of genes as expected in good quality cells (Supplementary Fig. 1 A). Differences remained in the distributions of mitochondrial and ribosomal RNA percentages, even after applying the respective thresholds (Supplementary Figures C—D), and no differences were observed between groups in terms of the number of genes or reads per cell (Supplementary Figures *E*-F). Nevertheless, cells with low number of genes detected (⟨300) and high number of molecules detected (>3000) were excluded in order to avoid the inclusion of uninformative and/or doublet cells in the analyses, these thresholds were decided based on the distribution in Supplementary Figs. 1E-F.

After applying all quality control filters, 82,698 cells remained. The gene profiling of these cells were normalized, scaled and the highest variable genes were selected using the Seurat R package (Butler et al., 2018). To integrate the different samples into a common dimensional space, reciprocal principal component analysis (RPCA) was applied. Based on the RPCA results, a shared nearest neighbor (SNN) graph was constructed. Clustering was performed using the Louvain algorithm across multiple resolutions. To determine the optimal resolution, and thus the number of clusters, the stability of clusters across increasing resolutions was evaluated (Zappia and Oshlack, 2018). The resolution of 0.5, which yielded eleven stable clusters, was selected, as it provided the highest stability before cell assignments began to fluctuate significantly at higher resolutions.

2.2. Single-nuclei RNA-Seq analysis of S. senegalensis male gonads identified the major cell types

Cell cluster annotation was performed based on manual inspection of cell type-specific markers (Supplementary Table 1) and pathway enrichment analysis of zebrafish MgSigDB (Liberzon et al., 2011) selected gene sets (Supplementary Table 2). In the t-SNE representation (Fig. 1A), all eleven clusters are clearly separated into the two-dimensional space. The heatmap of the top ten cell type markers (Fig. 1B) shows distinct expression patterns for each cluster, supporting their specific identities.

We identified two clusters with highly similar expression profiles (light brown and grayish blue clusters in Fig. 1B). Both displayed elevated expression of genes associated with stem cell maintenance and self-renewal, such as the transcription factors *sox1a*, *grin2aa*, and *prdm16*, among others. Gene set enrichment analysis (GSEA) revealed that both clusters share enriched pathways related to synaptic signaling

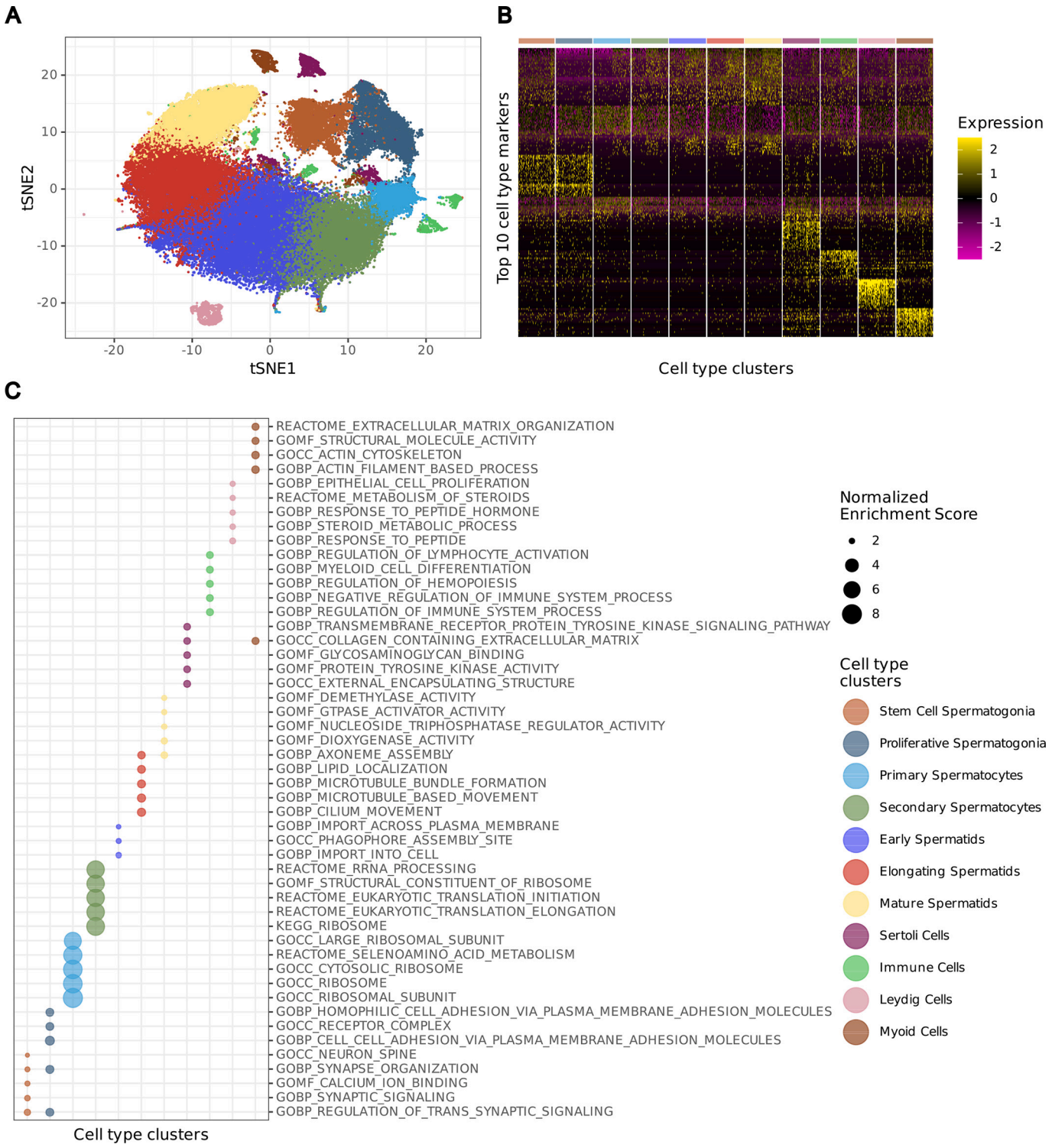

Fig. 1. Cell type identification and functional characterization in snRNA-Seq of male gonad of *Solea senegalensis*. (A) t-SNE plot based on the top 50 principal components derived from the 2000 most variable genes, cells are colored by identified cell type clusters. (B) Heatmap of the top 10 marker genes for each identified cell type cluster. Marker gene expression levels are scaled (*Z*-scores), with yellow indicating high expression and magenta indicating low expression. (C) Top 5 most enriched biological pathways for each cell type cluster (NES > 0 and q-value <0.1). The size of each dot represents the normalized enrichment score (NES), while the color indicates the corresponding cell type. Pathways are sorted by cell types. (For interpretation of the references to color in this figure legend, the reader is referred to the web version of this article.)

(Fig. 1C). Although spermatogonia do not participate in synaptic signaling in the classical neuronal sense, elements of these pathways, such as neurotransmitters, receptors, and associated signaling proteins, may play a role in cell communication within the gonadal environment. Notably, the grayish blue cluster showed enrichment in functions related to cell-cell adhesion and receptor complexes (Fig. 1C). Based on these observations, the light brown cluster likely represents spermatogonial stem cells, whereas the grayish blue cluster may comprise committed spermatogonia, which begin the differentiation process through strong interactions with Sertoli cells.

The five clusters with the largest number of cells are located at the center of the t-SNE plot (Fig. 1A) and exhibit a continuous marker expression gradient (Fig. 1B). The light blue cluster is characterized by high expression of ribosomal proteins, indicative of extensive protein synthesis, a hallmark of actively dividing cells. GSEA confirmed enrichment in ribosome-related processes and oxidative phosphorylation (Fig. 1C), consistent with rapid cell proliferation and preparation for meiotic entry, features typical of primary spermatocytes. The dark green cluster also maintains high ribosomal protein expression along with translation factors, such as *eef1b2*, suggesting ongoing cell growth and readiness for meiosis. In this cluster, translational regulation and ribosome biogenesis are the most enriched pathways, along with pathways responsive to amino acid availability, hallmark of mid or secondary spermatocytes. The dark blue cluster appears to represent cells transitioning from late meiosis to early spermatids. It shows upregulation of genes related to post-transcriptional regulation (*cpeb1b*, *mbnl1*, *nova1*) and chromatin remodeling (*brdt*, *arid5a*, *kdm6ba*), indicating ongoing postmeiotic processes. Enrichment in pathways related to membrane trafficking and autophagy (Fig. 1C) reflects the initiation of cellular remodeling, including uptake of essential metabolites and membrane components for flagellum and acrosome formation, while unnecessary organelles are being degraded. The red cluster is enriched in genes involved in cytoskeleton regulation and cell morphology (*myo10*, *arhgap21b* or *arhgap39*), as well as spermatid structural remodeling (*enah* or *spata17*). Enrichment in cilium movement, lipid location, and axoneme assembly pathways (Fig. 1C) further supports its identification as elongating spermatids undergoing significant morphological changes. The yellow cluster continues to express structural remodeling but also shows markers associated with sperm maturation and acrosome development (*dcst1*, *cadm3* or *tspan4a*). Functional enrichment in GTPase cycle and phosphatase activity suggest these cells are undergoing terminal remodeling, typical of late spermatids completing spermiogenesis (Fig. 1C).

The remaining clusters correspond to non-germline male gonad cell types. Sertoli cells (purple cluster) are identified by enrichment in structural, signaling and adhesion-related pathways (Fig. 1C), including the key marker *nr5a2*, which encodes a nuclear receptor essential for Sertoli cell function. Immune cells (light green cluster) are characterized by immune-related pathways associated with both lymphoid and myeloid lineages (Fig. 1C). Specific markers include *ptprc* (a pan-leukocyte antigen), *cd74b* (a B-cell marker), and *cd68* (a macrophage marker), among others. Leydig cells (pink cluster) are identified by pathways involved in steroid biosynthesis and hormone production (Fig. 1C). Marker genes such as *star* (steroidogenic acute regulatory protein), *ar* (androgen receptor), and *hsd11b2* (involved in steroid metabolism) confirm this identity. The brown cluster likely represents peritubular myoid cells or other structural cells contributing to the extracellular matrix (ECM) maintenance and testicular integrity. The expression of *tpm1*, *col6a3*, and *cald1b*, genes involved in smooth muscle function and ECM composition, supports this allocation. Enriched pathways also align with structural roles in supporting seminiferous tubules and facilitating sperm transport (Fig. 1C).

2.3. Trajectory analysis based on single-nuclei RNA-Seq molecular data revealed a spermatogenesis differentiation trajectory from marker-annotated spermatogonial stem cell to mature spermatids

Germline cell annotation was not an easy task based on functional markers, first due to the lack of functional annotation for many *S. senegalensis* genes that appears as strong markers of many of the clusters but without known function, and second because the spermatogenesis is a continuous process where frontiers between cell types are hard to define and thus some markers may overlap similar cell types. Therefore, in order to verify the existence of a transcriptional continuum between stem cell spermatogonial cells and the mature spermatids, germline cells were selected from the previous analyses and a trajectory inference was performed using Monocle3 (Trapnell et al., 2014).

The analysis revealed one single significant trajectory, without branches, flowing from the stem cell spermatogonial cluster to the mature spermatids cluster (Fig. 2A), as defined by the functional marker-based annotation in the previous analysis. To define the sequence of regulatory molecular changes driving the cell differentiation along spermatogenesis, four principal coregulated gene modules were identified (Fig. 2B). The functionality of these four modules were tested based on gene overrepresentation analysis on MgSigDB selected gene sets (Supplementary Table 3). Three of these modules (1, 2 and 4 in Fig. 2C) showed significant overrepresented pathways (q-value <0.1 and enrichment score > 0). Module 4 was overexpressed in spermatogonial cells with a peak at the proliferating spermatogonia; then its expression decreased after primary spermatocytes (Fig. 2B), showing pathways related to ribosomal biogenesis and rRNA maturation, consistent with increased translational demand during early differentiation. Additionally, responsiveness to fibroblast growth factors and regulation of ubiquitin-mediated proteolysis highlight active engagement with proliferative and survival signals, positioning these cells for mitotic expansion and lineage commitment (Fig. 2C). Module 2 peak corresponds to spermatocytes; the expression of cluster-specific markers increases since proliferative spermatogonia and decreases at early stages of spermatid maturation (Fig. 2B). Unexpected enrichment of steroid hormone biosynthesis and glucocorticoid metabolism pathways in spermatocytes suggests that these cells may transiently engage in local steroidogenic activity or modulate their sensitivity to hormonal process. Additionally, enrichment of potassium channel regulation indicates active ionic remodeling during meiotic progression, consistent with known changes in membrane dynamics and volume regulation (Fig. 2C). Module 1 defines the last stages of the differentiation, the expression initiates at secondary spermatocytes, reaching its peak at early spermatids but maintaining a high expression in all spermatid clusters (Fig. 2B). In this module, pathways related to oxidative phosphorylation and mitochondrial ATP synthesis were enriched, consistent with the increased energy demands associated with sperm motility. Additionally, omega peptidase activity suggests active proteolytic remodeling during the final stages of spermiogenesis (Fig. 2C).

2.4. Captive-bred males showed overrepresentation of spermatogonial cell stages compared to wild-bred males

There are different types of infertility, and some may be associated with alterations in the cellular composition along spermatogenesis, such as in cases of azoospermia or oligospermia. To investigate cell type composition through differentiation, we visualized overall cell type density using t-SNE dimensionality reduction (Fig. 3A) and represented individual cell type proportions using bar plots (Fig. 3B). Both analyses revealed overrepresentation of spermatogonial cells, particularly proliferative spermatogonia, and a depletion of mature spermatids in CB males. To validate the observed imbalance in cell proportions, we performed bulk RNA-Seq analysis on independent biological samples. GSEA was conducted using bulk RNA-Seq differential analysis results and the top 100 marker genes for each germ cell type involved in spermatogenesis. CB animals showed a significant depletion of spermatid markers (NES < -2), with p-values $<$5e-10 across all three identified spermatid subtypes, as well as an enrichment in spermatogonial markers (NES $\sim$ 1), but not statistically significant (Supplementary Table 4). Notably, a clear transition from marker enrichment to depletion across differentiation stages was evident when plotting the running enrichment score for all cell types (Fig. 3C).

The overrepresentation of spermatogonial cell types in CB animals suggests the existence of molecular dysregulation that impairs the commitment of spermatogonial cells to the spermatogenic differentiation process. To investigate which molecular pathways may be involved in this impairment, differential expression analysis and GSEA were performed on the stem cell and proliferative spermatogonial clusters,

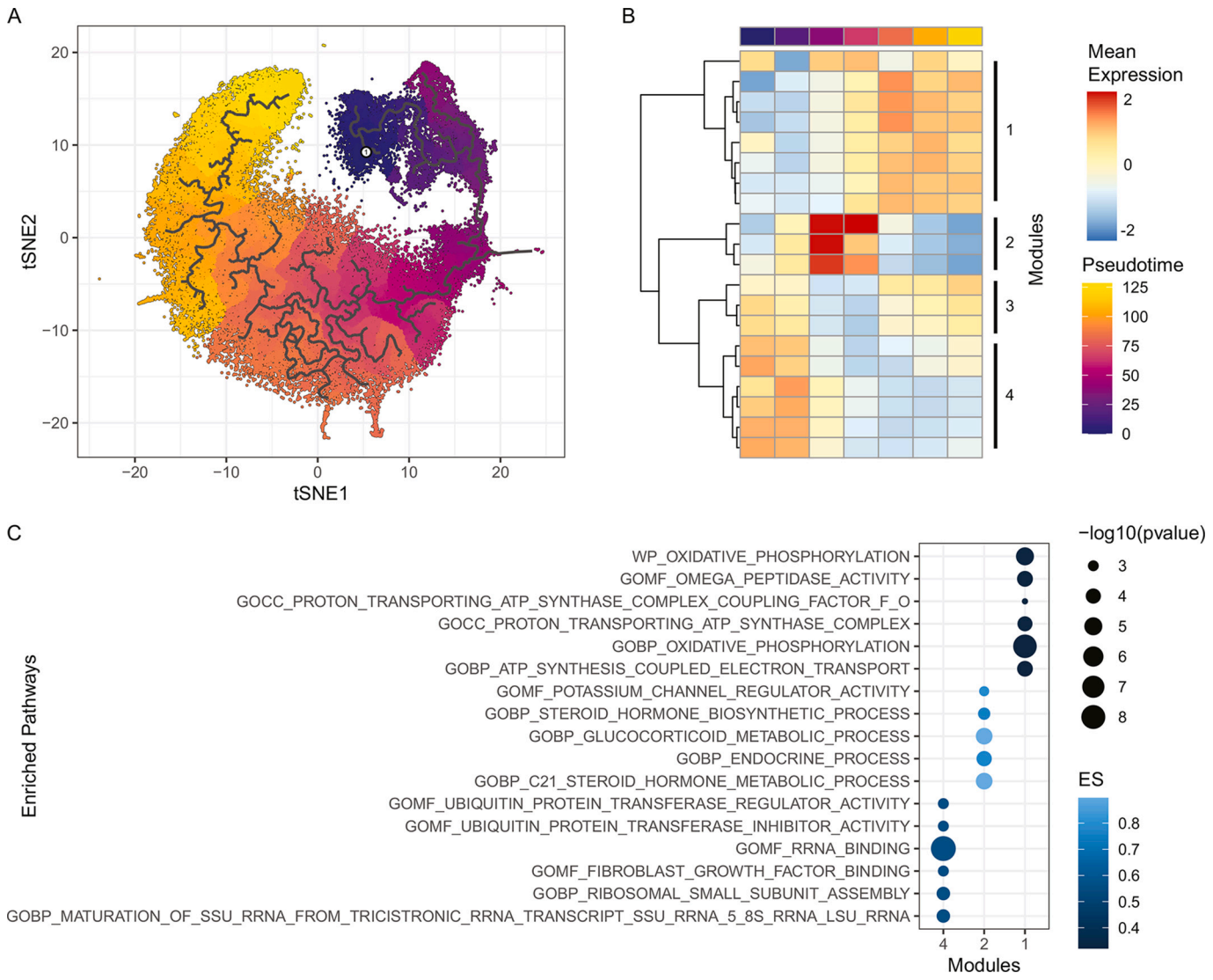

Fig. 2. Pseudotime trajectory and module-specific gene expression dynamics on germline male gonad cells. (A) t-SNE plot showing the distribution of cells along pseudotime, colored by pseudotime progression from purple (early) to yellow (late). Black lines represent the inferred trajectory path across the cell population. (B) Heatmap showing the expression patterns of genes grouped into co-expression modules across pseudotime. Rows correspond to gene modules, and columns represent each of the identified cell types. Gene expression is averaged and scaled, and the color bar above the heatmap indicates average pseudotime progression per cell type. (C) Top 5 most overrepresented pathways for the genes contained in each gene module identified during trajectory analysis (ES $>$ 0 and q-value $<$0.1). The size of the dots represents the statistical significance of enrichment (−log10(*p*-value)), while the color intensity denotes the enrichment score (ES), with lighter colors indicating stronger enrichment. (For interpretation of the references to color in this figure legend, the reader is referred to the web version of this article.)

comparing CB and WB animals. The analysis revealed two major groups of downregulated pathways in CB spermatogonial cells: those related to synaptic and neural processes, and those associated with adhesion and cytoskeletal dynamics (Fig. 3D and Supplementary Table 5). As previously mentioned, although synaptic and neuronal terms are classically associated with the nervous system, similar mechanisms are active in spermatogonial cells, particularly in cell communication and differentiation. Their downregulation may therefore indicate impaired cell communication, potentially disrupting the differentiation process. Additionally, the downregulation of adhesion and cytoskeleton-related pathways may compromise the interaction between spermatogonial and Sertoli cells, which is essential for niche maintenance and proper differentiation. In contrast, the upregulated pathways in CB spermatogonial cells were mainly associated with ribosome structure, translation, and co-translational protein targeting, suggesting a shift in cellular activity toward increased protein synthesis.

2.5. *Spermatogonia-Sertoli cell in-silico predicted interactions are markedly dysregulated in captive-bred males*

To further investigate the potential role of downregulated cell-cell communication during spermatogonial stages, NicheNet (Browaeys et al., 2020) was employed to assess intercellular signaling in proliferative spermatogonia. Since the NicheNet cell-cell communication network is based on human and mouse data, only orthologous genes between *S. senegalensis* and humans, as identified in the NCBI orthologs database (Sayers et al., 2025a), were included in the analysis. It is important to note that these results represent *in-silico* predictions based of potential ligand-receptor interactions from a human database, and while they provide valuable hypotheses, functional validation in *S. senegalensis* will be required to confirm their biological relevance. Briefly, NicheNet calculates the prior interaction potential of ligand-receptor pairs using biological knowledge gathered from multiple databases. It then estimates ligand activity based on how well the expression of a ligand in ligand-producing cells (senders) can explain

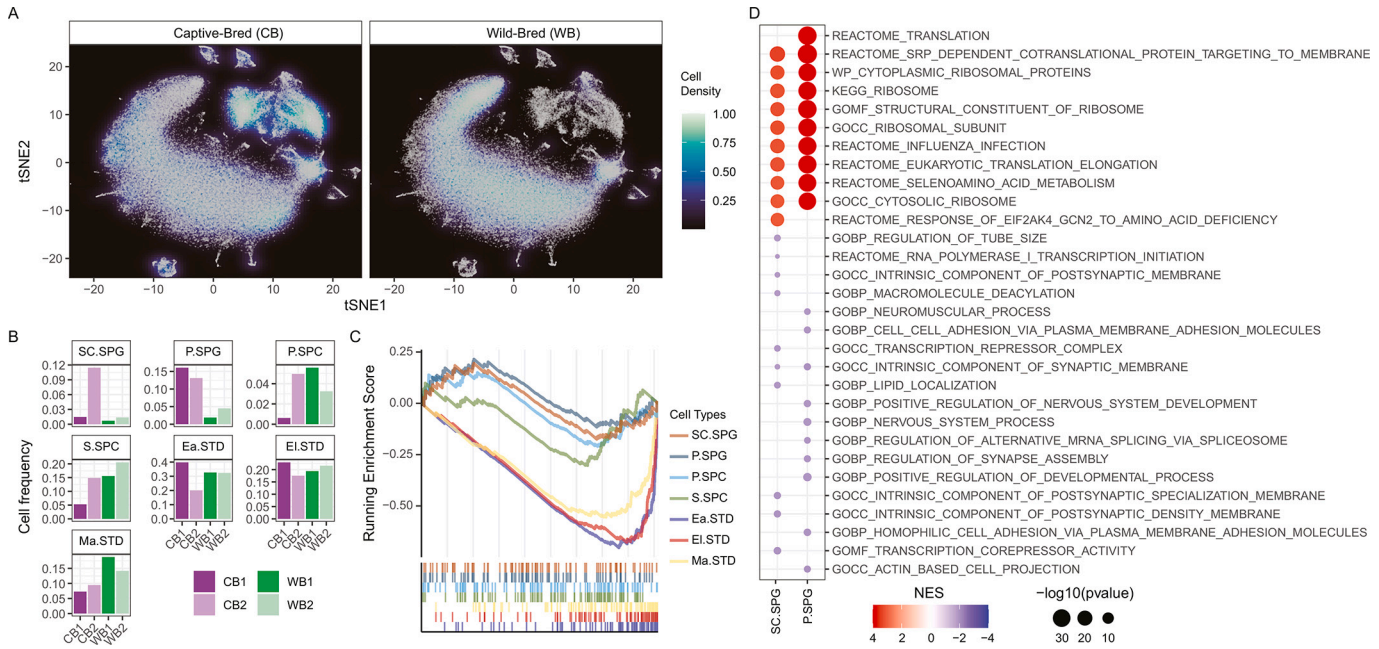

Fig. 3. Altered cell type composition and cell-cell interactions in gonads from CB males.
(A) t-SNE projections of snRNA-Seq from male gonads of CB and WB individuals, showing cell density. (B) Bar plots representing the relative frequency of each annotated germ cell type across biological replicates for both CB and WB groups. Cell types are SC.SPG (stem cell spermatogonia), P.SPG (proliferative spermatogonia), P.SPC (primary spermatocytes), S.SPC (secondary spermatocytes), Ea.SPD (early spermatids), El.SPD (elongating spermatids), Ma.SPD (mature spermatids). (C) GSEA results based on differential analysis of male gonad bulk RNA-Seq data between CB and WB individuals. Enrichment scores were calculated using the top 100 marker genes for each germ cell identified in the scRNA-Seq. (D) Dot plot showing the top five upregulated and downregulated pathways from the GSEA analysis comparing CB and WB groups in stem cell spermatogonia (SCSg) and proliferative spermatogonia (PSg). Dots are colored by normalized enrichment score (NES) and sized by -log10(q-value).

observed expression changes in target genes within the receiver cell population. Finally, it computes a regulatory potential score, representing the likelihood that a ligand influences a downstream target gene through intermediate signaling and transcriptional networks.

A differential expression analysis of target genes in proliferative spermatogonia from the NicheNet database revealed a substantial downregulation in CB animals (Fig. 4A), with over 50 % of target genes being downregulated. This observation is consistent with our previous findings linking gene downregulation to impaired cell-cell communication. These downregulated target genes were subsequently used for ligand activity calculations. Sertoli, Leydig, myoid, and immune cells were considered potential senders interacting with spermatogonial receptors. Accordingly, the database was filtered based on the expression of ligands in senders and receptors in the receiver cell. Ligand-receptor pairs were then selected based on this filtering, and their prior interaction potential was estimated. Among these, the receptor with the highest number of predicted interactions affecting downregulated target genes was the epidermal growth factor receptor (*egfr*) (Fig. 4B), a gene known to play a crucial role in spermatogonial stem cell differentiation.

Then, ligand-producing cell types were identified by comparing the expression levels of each ligand across all potential senders. A ligand was considered specifically produced by one sender if it showed a mean expression level higher than the mean plus one standard deviation across all potential senders. This analysis showed that nearly half of the ligands (12 out of 25) were predominantly expressed in Sertoli cells. Consistently, nearly half of the target genes affected by these interactions with spermatogonial cells receptors (75 out of 152) were also mediated by these Sertoli cell-derived ligands (Fig. 4C). The target genes with the highest number of regulatory interactions originating from Sertoli cells were *bcl2*, *bcl2l1*, and *cdk6*, each with eleven interactions, followed by *lef1* and *smad7*, each with ten. Additionally, although involved in fewer interactions, key genes involved in spermatogenesis, such as *ar* (androgen receptor), were also potentially affected by ligand-receptor dysregulation (Fig. 4C). Once ligand activity was inferred based on target gene downregulated in the proliferative spermatogonia of CB animals, *angptl4* emerged as the ligand with the highest activity (Fig. 4D). It is almost exclusively expressed in Sertoli cells (Fig. 4E) and exhibits a strong regulatory potential over many of the genes that are also highly targeted by other Sertoli cell-produced ligands (Fig. 4F). These include *lef1*, the target gene with the highest regulatory potential; *bcl2*, the gene influenced by the greatest number of ligands with positive regulatory potential; as well as other key genes such as *ar* and *slc1a5*, the latter being the second highest in regulatory potential among the target genes.

3. Methods

3.1. Biological sample acquisition

Adult CB and WB males were sacrificed by decapitation at the Sea Eight farm (Safiestela, Portugal) following the ethical procedures of the company. Both gonads from each animal were dissected and immediately flash-frozen in liquid nitrogen, to be then stored at −80 °C until their use for the single-nuclei protocol. One testicle from each individual was used for snRNA-Seq and the other for bulk RNA-Seq. In total, for snRNA-Seq 2 CB and 2 WB animals were available, while for bulk RNA-Seq the analysis was performed on 3 CB and 6 WB animals.

3.2. Molecular profiling

3.2.1. Single-nuclei RNA-Seq library preparation

Nuclei were extracted following a published protocol (Krishnaswami et al., 2016) with small modifications for use in non-standard vertebrate species (Murat et al., 2023). Briefly, the frozen gonads were homogenized using a micropestle in 400 μL ice-cold homogenization buffer (250 mM sucrose, 25 mM KCl, 5 mM MgCl2, 10 mM Tris-HCl [pH 8], 0.1 %

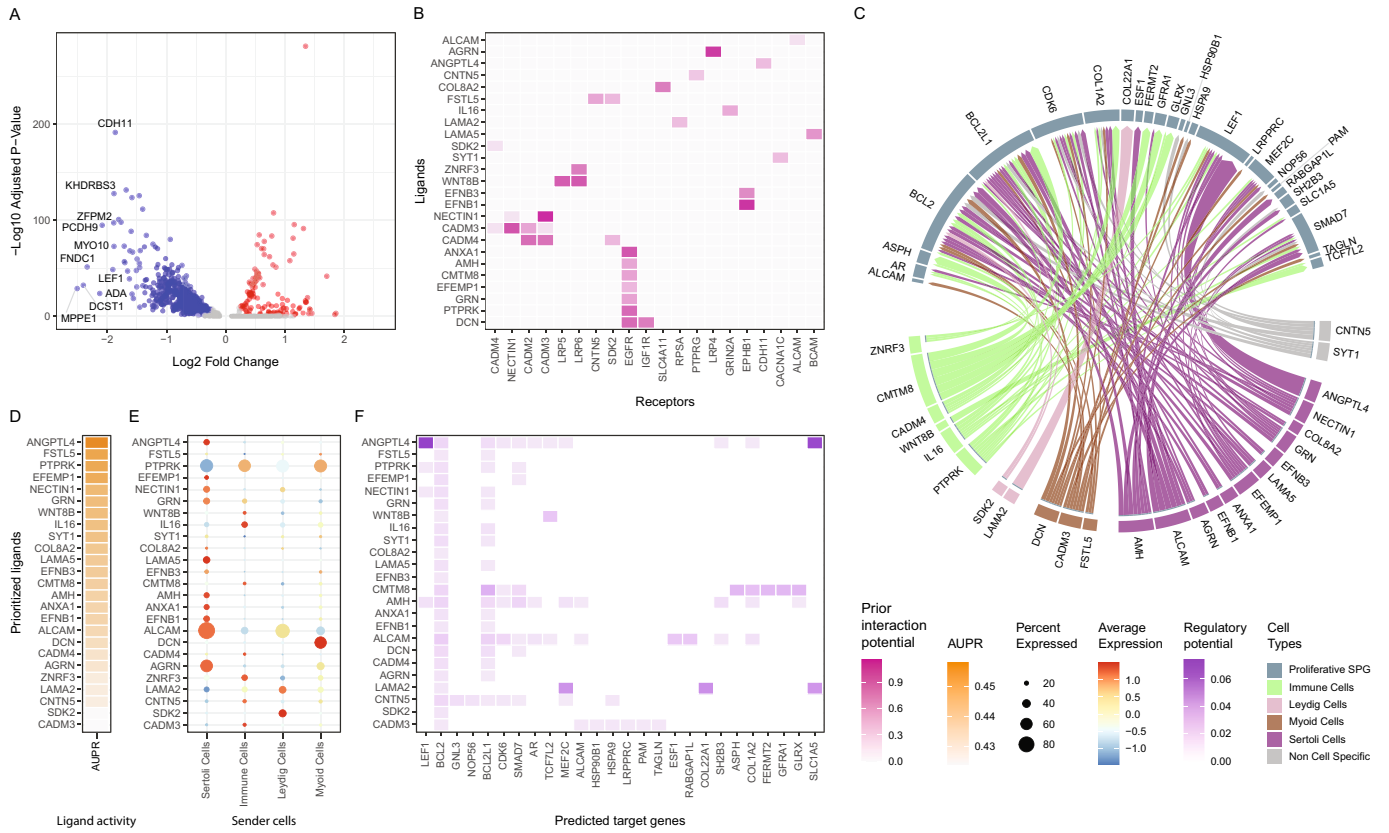

Fig. 4. Cell-cell communication networks reveal downregulated target genes downstream of ligand–receptor interactions. (A) Volcano plot showing differentially targeted genes downstream of ligand–receptor interactions between CB and WB animals. Significantly upregulated genes are shown in red, and downregulated genes in blue. (B) Heatmap of ligand-receptor pairs upstream of downregulated target genes in CB animals, highlighting prior interaction potential. (C) Circos plot displaying inferred ligand-target networks. Links represent prioritized signaling interactions from sender to receiver cells, colored by the predominant ligand-expressing sender cell type. P.SPG stands for proliferative spermatogonia. (D) Heatmap ranking ligands by their activity scores (AUPR), based on the downregulated target genes. (E) Dot plot showing ligand expression across sender cell types. Dot size represents the percentage of cells expressing each ligand, while color denotes average expression level. (F) Heatmap showing the regulatory potential of ligands on predicted target genes. (For interpretation of the references to color in this figure legend, the reader is referred to the web version of this article.)

IGEPAL, 1 μM dithiothreitol [DTT], 0.4 U/μL Murine RNase Inhibitor [New England BioLabs, M0314L], and 0.2 U/μL SUPERase-In [Ambion, AM2694]). The homogenates were triturated gently using a p1000 tip 10 times, incubated on ice for 5 min and then centrifuged at 100*g* for 1 min at 4 °C to pellet any unlysed tissue chunks. The supernatant was transferred into another 1.5 mL Eppendorf tube and centrifuged at 400*g* for 4 min at 4 °C to collect nuclei. The nuclei were washed twice in 400 μL homogenization buffer and strained using a 40 μm Flowmi strainer (Sigma, BAH136800040) during the second wash step to remove nuclei aggregates. The final nuclei pellet was resuspended in 30–50 μL Nuclei Bufer (10× Genomics, PN-2000207). To estimate the nuclei concentration, nuclei aliquots were diluted in phosphate-buffered-saline (PBS) with Hoechst and propidium iodide (PI) DNA dyes and counted on Countless II FL Automated Cell Counter (Thermo Fisher Scientific, RRID: SCR_020236). The Chromium Next GEM Single Cell 3' Reagent Kits v3.1 (PN-1000121, PN-1000120, and PN-1000213) were used to make snRNA-seq libraries. Libraries were quantified on a Qubit Fluorometer (Termo Fisher Scientifc; RRID: SCR_018095) and quality checked on a Fragment Analyzer (Agilent; RRID: SCR_019417). Finally, snRNA-seq libraries were sequenced on an Illumina NovaSeq 6000 platform, generating 150 bp paired-end reads.

3.2.2. Bulk RNA-Seq library preparation

After sample thawing, total RNA was extracted and purified using the miRNeasy Kit (QIAGEN). RNA integrity and quantity were evaluated in a Bioanalyzer (Bonsai Technologies, Madrid, Spain) and in a NanoDrop® ND-1000 spectrophotometer (NanoDrop® Technologies Inc., Wilmington, DE, USA). RNA samples were delivered to Novogene (UK) for library preparation using NEBNext Ultra Directional RNA Library Prep Kits for Illumina and sequenced using an Illumina NovaSeq S4 platform to generate 150 bp paired end reads.

3.3. Statistical analysis

3.3.1. Single-nuclei RNA-Seq quality control and processing

The *S. senegalensis* IFAPA_SoseM_1 genome assembly (GCF_019176455.1) and corresponding gene annotation were downloaded from the NCBI RefSeq Genome Database (Goldfarb et al., 2025). A CellRanger (v8.0) (CellRanger, 2025) reference was constructed, and FASTQ files were subsequently processed, aligned, and annotated. Additionally, CellRanger filtered cell barcodes to remove empty droplets, cellular debris, and ambient RNA, retaining barcodes that represented true cells.

For downstream analysis, cells were retained if they exhibited more than 500 counts, and genes were retained if they had more than 3 counts in at least 50 cells. Additional filtering criteria based on mitochondrial and ribosomal gene percentages, as well as total counts and feature counts per cell, were applied as follows: mitochondrial gene percentage < 10 %, ribosomal gene percentage > 1 %, gene count per cell >300, and total counts per cell <3000.

Cell cycle scores were calculated using the Seurat R package (v5.1) (Butler et al., 2018), employing predefined reference gene sets (Tirosh et al., 2016). Gene expression data were normalized and scaled using Seurat, and the top 2000 most variable features were identified using the

variance-stabilizing transformation ("vst") method. Dimensionality reduction was performed using principal component analysis (PCA), retaining the first 50 principal components (PCs). Integration of snRNA-seq samples was carried out using reciprocal PCA (RPCA). Subsequently, t-distributed stochastic neighbor embedding (t-SNE) was applied to reduce the first 50 RPCA dimensions to two-dimensional space for visualization.

To identify the most stable clustering configuration, a k-nearest neighbor ($k-$NN) graph was constructed based on the first 50 RPCA dimensions to capture relationships between cells. Community detection using the Louvain algorithm was performed at multiple resolutions (0.05, 0.1–1.0 in increments of 0.1, 1.5, and 2.0). The resulting Louvain clustering resolutions were compared using the clustree R package (Zappia and Oshlack, 2018) to determine the optimal, most stable cluster configuration.

3.3.2. Bulk RNA-Seq quality control and processing

Briefly, raw reads quality was examined using FASTQC (Andrews, 2010) and adapters were trimmed using Trim Galore (Krueger, 2012), a wrapper tool of Cutadapt (Martin, 2011). Filtered reads were then mapped to the *S. senegalensis* genome using STAR (Dobin et al., 2013). For differential expression analysis, normalized transcript reads were filtered based on their expression, preserving only genes with a Transcript per Million Reads (TPM) value >5.

3.3.3. Functional and enrichment analyses

Functional interpretation of marker genes and differential expression analyses were conducted using Gene Set Enrichment Analysis (GSEA) and Overrepresentation Analysis (ORA) implemented in the ClusterProfiler R package (v4.12.6) (Wu et al., 2021). Orthologs of *S. senegalensis* genes in zebrafish were identified via NCBI Gene IDs and the NCBI ortholog database (Sayers et al., 2025b) using the Orthology.eg.db R package (v3.19.1). Zebrafish gene sets from the Molecular Signatures Database (MsigDB) (Liberzon et al., 2015), retrieved using the msigdbr R package (v7.5.1), were utilized for functional analyses. The gene sets included BIOCARTA, KEGG, PID, Reactome, WikiPathways, and Gene Ontology (GO) terms.

3.3.4. Single-nuclei trajectory analysis

Single-nuclei trajectory analysis was performed using Monocle3 (Trapnell et al., 2014), following the authors' guidelines. Cell clusters corresponding to stages within the spermatogenesis differentiation process were selected, and t-SNE RPCA embeddings from the complete dataset were utilized for this analysis. The trajectory root was programmatically defined, as recommended by the authors, within the spermatogonial stem cell cluster. To identify correlated gene modules, genes exhibiting variation across the trajectory were selected based on Moran's I spatial autocorrelation metric (q-value <1e-5). Louvain community detection was then applied to gene embeddings at multiple resolutions (1e-6, 1e-5, 1e-4, 1e-3, 1e-2, 1e-1) to determine the most stable partition, resulting in the identification of twenty co-regulated gene modules. These twenty modules were further grouped into four principal modules based on hierarchical clustering of average expression across modules and cell types identified in the analysis.

3.3.5. Differential and cell-cell interaction analyses based on in-silico orthology

Bulk RNA-Seq differential analysis was conducted using the R package DESeq2 (v1.38.1) (Love et al., 2014) comparing CB versus WB animals.

Single-nuclei RNA-seq differential expression analyses were performed using the Wilcoxon test implemented in Seurat. Cluster marker genes were identified by comparing cells within a cluster against all other cells, while functional differential analyses compared cells of the same cell type between different conditions (CB versus WB).

Cell-cell *in-silico* interaction analyses were performed using the NicheNet R package (v2.2.0) (Browaeys et al., 2020). Given that the cell-cell interaction database curated by the NicheNet authors only contains human and mouse datasets, this analysis was restricted to *S. senegalensis* genes with human orthologs identified via NCBI Gene IDs and the NCBI ortholog database (Sayers et al., 2025b) using the Orthology.eg.db R package (v3.19.1).

4. Discussion

Selective breeding programs in aquaculture have proven highly effective across numerous orders of finfish and shellfish, enabling producers to meet consumer demand competitively while maintaining ecological integrity and preserving biodiversity (Azra et al., 2022). Flatfish have been successfully bred in captivity worldwide, achieving significant economic outcomes. However, for *S. senegalensis*, one of the most promising European flatfish species due to its flesh quality and high market value (Morais et al., 2016), genetic breeding programs aimed at enhancing productivity face important challenges related to reproductive constraints on farms. This has primarily to do with CB males, which produce low and variable sperm volumes (Beirão et al., 2011; Cabrita et al., 2006; Ramos-Júdez et al., 2021). Furthermore, these males are unable to perform the typical courtship with females (Morais et al., 2016; Riesco et al., 2019), which suggests a connection with their low sperm production. Neither CB females nor WB males maintained under captivity conditions exhibit reproductive limitations (Fatsini et al., 2020; Martín et al., 2019), which prompts to focus the problem on CB males.

Previous studies employed gonadal bulk RNA-Seq and methylation profiling, they revealed numerous differences between CB and WB males and identified critical pathways associated with male gonadal development, including MAPK signaling, Wnt signaling pathway, olfactory receptors, focal adhesion, or ECM-receptor interactions, among others (Anaya-Romero et al., 2025; Ramírez et al., 2025; Ramírez et al., 2024). However, bulk molecular analyses in complex biological samples containing diverse cell types and variable cell numbers, without an effective deconvolution signature matrix, provide limited information regarding the specific cell types in which dysregulation occurs and fail to capture the complete molecular landscape underlying infertility (Stuart and Satija, 2019). Thus, to elucidate the molecular mechanisms underlying infertility in captive-bred males at the cellular level, gonadal tissue from adult CB and WB males was collected and subjected to snRNA-Seq profiling.

Single-nuclei RNA sequencing enabled the identification of eleven distinct cell clusters within the gonads of *S. senegalensis*. These clusters encompassed multiple stages of the spermatogenesis process, including spermatogonial stem cells, differentiating spermatogonia, spermatocytes, and spermatids. Additionally, we identified supporting cell types such as Sertoli cells, endocrine cell populations including Leydig cells, and, at lower abundances, structural and immune cell populations within the gonadal environment (Qian et al., 2022; Yang et al., 2024). All identified cell clusters exhibited the expression of well-established marker genes, confirming their cellular identities within the dataset. However, a substantial number of genes demonstrated high cluster specificity beyond known markers, suggesting their potential as candidate genes for further functional characterization. These cluster-specific genes could serve as valuable tools for developing accurate signature matrices for future deconvolution analyses in bulk transcriptomics, aiding the monitoring of gonadal status and reproductive health in *S. senegalensis* and related species. Although cell-type identities were inferred from snRNA-seq profiles, further validation using additional experimental approaches will be essential to confirm and refine these assignments in future studies.

Trajectory analysis of spermatogenesis further elucidated the key dynamic molecular pathways underlying the differentiation process from spermatogonial stem cells to mature spermatids. Pathways related to ribosome biogenesis, growth factor signaling, and ubiquitination

were highly active during the spermatogonial and early spermatocyte stages, reflecting the intense proliferative and translational demands of these phases. Notably, the trajectory analysis revealed enrichment of small ribosomal subunit genes together with FGF signaling in proliferating spermatogonia, consistent with their role in mRNA scanning and initiation during rapid mitotic activity. In contrast, the cell-type marker analysis highlighted the overexpression of large ribosomal subunit genes in primary spermatocytes, supporting enhanced peptide bond formation and translation of meiosis-specific proteins. These complementary patterns underscore distinct translational requirements across germ cell states: initiation-focused activity in spermatogonia and elongation-focused activity in spermatocytes. These processes declined as cells transitioned into later spermatocyte stages, where we observed a marked enrichment in endocrine and hormone biosynthetic pathways, reflecting the critical role of steroid hormones in regulating meiosis and germ cell maturation (Marín-Juez et al., 2013). In the spermatid clusters, pathways associated with oxidative phosphorylation and ATP synthesis were prominently upregulated, aligning with the increased energy demands required for chromatin condensation, flagellar development, and cellular remodeling during the final stages of spermiogenesis (Castro-Arnau et al., 2022). Collectively, these findings highlight the dynamic and stage-specific molecular landscape of spermatogenesis in *S. senegalensis*, providing a foundational framework for understanding the molecular basis of male fertility in this species.

Among the potential causes of male infertility, some can be identified by examining the distribution of cells across the different stages of spermatogenesis. In the case of CB *S. senegalensis* males, we observed the presence of all spermatogenic cell types. However, their proportions differed markedly from those in WB counterparts. This indicates that male infertility in CB individuals is not due to a complete arrest of the spermatogenesis process but rather to a limitation in the number of cells successfully completing differentiation. Specifically, undifferentiated cell types, such as spermatogonial stem cells and proliferative spermatogonia, were overrepresented in CB males, while mature spermatids were 2–3 times less abundant compared to WB males. This skewed distribution suggests that the molecular disruptions underlying impaired reproductive success in captivity result in oligospermia, characterized by reduced numbers of mature sperm cells despite the continuation of spermatogenesis. It is noteworthy that while in vitro fertilization using sperm from CB males is technically feasible, the low sperm yield makes it economically impractical for implementation in large-scale breeding programs (Beirão et al., 2011; Cabrita et al., 2006; Ramos-Júdez et al., 2021).

To elucidate the molecular and endocrine mechanisms constraining the completion of spermatogenesis in captivity, we performed a differential analysis of spermatogonial clusters between CB and WB *Solea senegalensis* males. The results revealed a marked downregulation of molecular pathways related to cell-cell communication and cell adhesion processes in CB males, consistent with previous findings at the bulk RNA-Seq level (Anaya-Romero et al., 2025; López-Fortún et al., 2025). Due to limited annotation of fish-specific genes involved in cell-cell communication and the absence of experimentally validated ligand-receptor databases in teleosts, our analysis relied on known human orthologs to predict *in-silico* potential ligand-receptor interactions. Strikingly, more than 50 % of the predicted downregulated signaling pathways specifically involved Sertoli cell to proliferative spermatogonial cell interactions, indicating a potential impairment in this communication, which is crucial for the progression of spermatogonial differentiation. Sertoli cells are the only somatic cells in direct contact with spermatogonial cells, and proper cell-cell communication is essential for testis formation and spermatogenesis (Ni et al., 2019).

Among the ligand-receptor pairs predicted to be implicated, several ligands known to be highly expressed in Sertoli cells, including *nectin1*, *efnb1*, *efnb3*, *agrn* and *lama5*, were identified. These ligands are well-established mediators of Sertoli-spermatogonial adhesion and signaling. Additionally, Anti-Müllerian Hormone gene (*amh*), critical for male gonad development and Sertoli cell maturation, was also identified as an affected ligand in our cell-cell communication analysis. On the receiving end of these impaired interactions, genes associated with the self-renewal and maintenance of spermatogonial stem cells, such as *gfra1*, as well as *lef1* and *tcf7l2* (Wnt signaling mediators), were notably impacted. Moreover, ar (androgen receptor), a key regulator of spermatogenesis progression, was also identified among the affected downstream targets. Interestingly, while some identified genes have not been directly associated with spermatogenesis, they may still play important roles in this context. Notably, *angplt4* exhibited the highest predicted ligand activity in our analysis, suggesting a potential involvement in Sertoli-germ cell communication and gonadal function that warrants further investigation.

In addition, *bcl2* and *bcl2l1* emerged as the two genes predicted to be regulated by the highest number of interactions. These genes are known to regulate spermatogonial survival and apoptosis under the influence of Sertoli-derived paracrine factors (Print and Loveland, 2000). The impaired regulation of bcl2 and bcl2l1 is particularly significant, as defective apoptotic processes in spermatogonial cells unable to progress through spermatogenesis may lead to their accumulation. This accumulation could, in turn, further disrupt Sertoli-spermatogonial interactions, creating a self-reinforcing loop that blocks progression to the subsequent stages of differentiation, thereby contributing to the oligospermia observed in CB males.

Further investigations will be required to elucidate how these Sertoli-spermatogonial interactions become initially impaired, leading to the accumulation of undifferentiated spermatogonial cells in CB males. Notably, the oligospermia observed in these animals does not occur during the acclimation of WB males to captive conditions (Martín et al., 2019; Riesco et al., 2019). This observation leads us to hypothesize that epigenetic processes occurring during *S. senegalensis* development under captive conditions may result in defective gonadal maturation of CB males. Supporting this hypothesis our dataset revealed that *amh* is overexpressed in CB Sertoli cells. In teleosts, *amh* plays a direct role in testis development and germ-cell regulation. *Amh* is expressed in Sertoli cells and stem cell spermatogonia, where *amh* restrains the spermatogonial proliferation and delays the entry into meiosis (Pfennig et al., 2015). This suggests that the persistent overexpression of *amh* in CB Sertoli cells reflects an immature Sertoli phenotype that is less supportive of spermatogenesis. In this context, *amh* overexpression likely acts as a brake on spermatogonial differentiation, contributing to the observed accumulation of spermatogonia and depletion of spermatids in CB males. This mechanistic clue points to an early disruption at the level of the spermatogonial stem cell niche, although definitive conclusions about timing will require longitudinal analyses across developmental stages.

Despite the limited number of individuals profiled in this study and the absence of species-specific ligand-receptor interaction databases, our single-nuclei transcriptomic analysis predicted defective Sertoli-spermatogonial interactions as a key molecular driver of oligospermia in CB *S. senegalensis* males. These impaired interactions involve critical genes associated with spermatogonial differentiation and apoptosis regulation, leading to the accumulation of undifferentiated, defective spermatogonial cells within the gonads. Given that the NicheNet framework is curated from human and mouse datasets, the ligand-receptor interactions reported here should be interpreted as in silico predictions based on orthology. These results are therefore hypothesis-generating, and functional validation of key pairs (e.g., *angptl4-egfr*) will be essential to confirm their role in the reproductive dysfunction observed in *S. senegalensis*. At the same time, our main conclusions emphasize consistent and biologically interpretable changes across cell types rather than exhaustive gene-level comparisons, and we acknowledge that future studies with larger cohorts will be required to fully capture inter-individual variability and further consolidate the molecular signatures identified here.

Overall, our findings provide molecular insights that build a working

hypothesis for understanding the reproductive dysfunction observed in CB males, and they offer a framework for future studies aimed at exploring the molecular and epigenetic mechanisms that may constrain the successful completion of spermatogenesis in captivity.

Supplementary data to this article can be found online at https://doi.org/10.1016/j.aquaculture.2025.743593.

CRediT authorship contribution statement

Guillermo Barturen: Writing – review & editing, Writing – original draft, Formal analysis, Data curation, Conceptualization. **Diego Robledo:** Writing – review & editing, Data curation. **Francisca Robles:** Writing – review & editing. **Rose Ruiz Daniels:** Writing – review & editing, Data curation. **Maialen Carballeda:** Writing – review & editing, Formal analysis. **Dorinda Torres-Sabino:** Writing – review & editing, Formal analysis. **Rafael Navajas-Pérez:** Writing – review & editing. **Paulino Martínez:** Writing – review & editing, Writing – original draft. **Carmelo Ruiz-Rejón:** Writing – review & editing, Funding acquisition, Conceptualization. **Roberto De la Herrán:** Writing – review & editing, Writing – original draft, Funding acquisition, Conceptualization.

Declaration of competing interest

Guillermo Barturen reports financial support was provided by Spanish Government. Roberto De la Herran reports financial support was provided by Regional Government of Andalucia. Paulino Martinez reports financial support was provided by Spanish Government. Paulino Martinez reports financial support was provided by Regional Government of Galicia. Dorinda Torres-Sabino reports financial support was provided by Regional Government of Galicia. Maialen Carballeda reports financial support was provided by Spanish Government. If there are other authors, they declare that they have no known competing financial interests or personal relationships that could have appeared to influence the work reported in this paper.

Acknowledgements

This work was supported by Proyectos Plan Operativo FEDER Andalucía 2021-2027 (C-EXP-159-UGR23), MICIU/AEI/10.13039/501100011033 project (PID2022-137821OB-C31) and by Consellería de Economía, Industria e Innovación e Consellería de Cultura, Educación, Formación Profesional e Universidades, Xunta de Galicia (ED431C 2022/33). DTS was supported by a regional research fellowship (Xunta de Galicia, 06_IN606D_2022_2693134), MC by a fellowship within the framework of the State Plan for Scientific, Technical and Innovation Research 2021-2023 (PID2022-137821OB-C31) and GB by MICINN, Juan de la Cierva-Incorporación (IJC2020-043364-I). Funding for open access charge: Universidad de Granada / CBUA.

Data availability

Single-nucleus RNA-Seq FASTQ and H5DF files are available in the GEO repository under GSE302378. Bulk RNA-Seq data are currently being prepared for a separate publication and are available upon request. These data will be made publicly available following publication.

References

Aliaga-Guerrero, M., Paullada-Salmerón, J.A., Piquer, V., Mañanós, E.L., Muñoz-Cueto, J. A., 2018. Gonadotropin-inhibitory hormone in the flatfish, *Solea senegalensis*: molecular cloning, brain localization and physiological effects. J. Comp. Neurol. 526, 349–370. https://doi.org/10.1002/cne.24339.

Anaya-Romero, M., Ramírez, D., Arias-Pérez, A., Rodríguez, M.E., Robledo, D., Rebordinos, L., 2025. Comparative transcriptomic profiling of gonads in *Solea senegalensis*: exploring sex, maturity, and origin variations. Aquaculture 604, 742461. https://doi.org/10.1016/j.aquaculture.2025.742461.

Andrews, S., 2010. Babraham Bioinformatics - FastQC A Quality Control tool for High Throughput Sequence Data [WWW Document]. URL. https://www.bioinformatics.babraham.ac.uk/projects/fastqc/. accessed 7.4.25.

Azra, M.N., Okomoda, V.T., Ikhwanuddin, M., 2022. Breeding technology as a tool for sustainable aquaculture production and ecosystem services. Front. Mar. Sci. 9. https://doi.org/10.3389/fmars.2022.679529.

Beirão, J., Soares, F., Herráez, M.P., Dinis, M.T., Cabrita, E., 2011. Changes in *Solea senegalensis* sperm quality throughout the year. Anim. Reprod. Sci. 126, 122–129. https://doi.org/10.1016/j.anireprosci.2011.04.009.

Bélteky, J., Agnvall, B., Bektic, L., Höglund, A., Jensen, P., Guerrero-Bosagna, C., 2018. Epigenetics and early domestication: differences in hypothalamic DNA methylation between red junglefowl divergently selected for high or low fear of humans. Genet. Sel. Evol. 50, 13. https://doi.org/10.1186/s12711-018-0384-z.

Benzekri, H., Armesto, P., Cousin, X., Rovira, M., Crespo, D., Merlo, M.A., Mazurais, D., Bautista, R., Guerrero-Fernández, D., Fernandez-Pozo, N., Ponce, M., Infante, C., Zambonino, J.L., Nidelet, S., Gut, M., Rebordinos, L., Planas, J.V., Bégout, M.-L., Claros, M.G., Manchado, M., 2014. De novo assembly, characterization and functional annotation of Senegalese sole (*Solea senegalensis*) and common sole (*Solea solea*) transcriptomes: integration in a database and design of a microarray. BMC Genomics 15, 952. https://doi.org/10.1186/1471-2164-15-952.

Browaeys, R., Saelens, W., Saeys, Y., 2020. NicheNet: modeling intercellular communication by linking ligands to target genes. Nat. Methods 17, 159–162. https://doi.org/10.1038/s41592-019-0667-5.

Butler, A., Hoffman, P., Smibert, P., Papalexi, E., Satija, R., 2018. Integrating single-cell transcriptomic data across different conditions, technologies, and species. Nat. Biotechnol. 36, 411–420. https://doi.org/10.1038/nbt.4096.

Cabrita, E., Soares, F., Dinis, M.T., 2006. Characterization of Senegalese sole, *Solea senegalensis*, male broodstock in terms of sperm production and quality. Aquaculture 261, 967–975. https://doi.org/10.1016/j.aquaculture.2006.08.020.

Castro-Arnau, J., Chauvigné, F., Gómez-Garrido, J., Esteve-Codina, A., Dabad, M., Alioto, T., Finn, R.N., Cerdà, J., 2022. Developmental RNA-Seq transcriptomics of haploid germ cells and spermatozoa uncovers novel pathways associated with teleost spermiogenesis. Sci. Rep. 12, 14162. https://doi.org/10.1038/s41598-022-18422-2.

CellRanger, 2025. WWW Document. URL. https://scicrunch.org/resolver/SCR_017344. accessed 6.28.25.

Chauvigné, F., Fatsini, E., Duncan, N., Ollé, J., Zanuy, S., Gómez, A., Cerdà, J., 2016. Plasma levels of follicle-stimulating and luteinizing hormones during the reproductive cycle of wild and cultured Senegalese sole (*Solea senegalensis*). Comp. Biochem. Physiol. A Mol. Integr. Physiol. 191, 35–43. https://doi.org/10.1016/j.cbpa.2015.09.015.

De la Herrán, R., Hermida, M., Rubiolo, J.A., Gómez-Garrido, J., Cruz, F., Robles, F., Navajas-Pérez, R., Blanco, A., Villamayor, P.R., Torres, D., Sánchez-Quinteiro, P., Ramirez, D., Rodríguez, M.E., Arias-Pérez, A., Cross, I., Duncan, N., Martínez-Peña, T., Riaza, A., Millán, A., De Rosa, M.C., Pirolli, D., Gut, M., Bouza, C., Robledo, D., Rebordinos, L., Alioto, T., Ruíz-Rejón, C., Martínez, P., 2023. A chromosome-level genome assembly enables the identification of the follicule stimulating hormone receptor as the master sex-determining gene in the flatfish *Solea senegalensis*. Mol. Ecol. Resour. 23, 886–904. https://doi.org/10.1111/1755-0998.13750.

De Silva, S., Nguyen, T., Ingram, B., 2008. Fish Reproduction in Relation to Aquaculture. Deakin University.

Dobin, A., Davis, C.A., Schlesinger, F., Drenkow, J., Zaleski, C., Jha, S., Batut, P., Chaisson, M., Gingeras, T.R., 2013. STAR: ultrafast universal RNA-seq aligner. Bioinforma. Oxf. Engl. 29, 15–21. https://doi.org/10.1093/bioinformatics/bts635.

Duarte, C.M., Marbá, N., Holmer, M., 2007. Ecology. Rapid domestication of marine species. Science 316, 382–383. https://doi.org/10.1126/science.1138042.

FAO, 2022. The State of World Fisheries and Aquaculture 2022. FAO.

Fatsini, E., González, W., Ibarra-Zatarain, Z., Napuchi, J., Duncan, N.J., 2020. The presence of wild Senegalese sole breeders improves courtship and reproductive success in cultured conspecifics. Aquaculture 519, 734922. https://doi.org/10.1016/j.aquaculture.2020.734922.

Gilannejad, N., Rønnestad, I., Lai, F., Olderbakk-Jordal, A.-E., Gottlieb Almeida, A.P., Martínez-Rodríguez, G., Moyano, F.J., Yúfera, M., 2021. Daily rhythms of intestinal cholecystokinin and pancreatic proteases activity in Senegalese sole juveniles with diurnal and nocturnal feeding. Comp. Biochem. Physiol. A Mol. Integr. Physiol. 253, 110868. https://doi.org/10.1016/j.cbpa.2020.110868.

Gjedrem, T., Baranski, M., 2009. Domestication and the application of genetic improvement in aquaculture. In: Gjedrem, T., Baranski, M. (Eds.), Selective Breeding in Aquaculture: An Introduction. Springer, Netherlands, Dordrecht, pp. 5–11.

Goldfarb, T., Kodali, V.K., Pujar, S., Brover, V., Robbertse, B., Farrell, C.M., Oh, D.-H., Astashyn, A., Ermolaeva, O., Haddad, D., Hlavina, W., Hoffman, J., Jackson, J.D., Joardar, V.S., Kristensen, D., Masterson, P., McGarvey, K.M., McVeigh, R., Mozes, E., Murphy, M.R., Schafer, S.S., Souvorov, A., Spurrier, B., Strope, P.K., Sun, H., Vatsan, A.R., Wallin, C., Webb, D., Brister, J.R., Hatcher, E., Kimchi, A., Klimke, W., Marchler-Bauer, A., Pruitt, K.D., Thibaud-Nissen, F., Murphy, T.D., 2025. NCBI RefSeq: reference sequence standards through 25 years of curation and annotation. Nucleic Acids Res. 53, D243–D257. https://doi.org/10.1093/nar/gkae1038.

Guerrero-Cózar, I., Gómez-Garrido, J., Berbel, C., Martínez-Blanch, J.F., Alioto, T., Claros, M.G., Gagnaire, P.-A., Manchado, M., 2021. Chromosome anchoring in Senegalese sole (*Solea senegalensis*) reveals sex-associated markers and genome rearrangements in flatfish. Sci. Rep. 11, 13460. https://doi.org/10.1038/s41598-021-92601-5.

Krishnaswami, S.R., Grindberg, R.V., Novotny, M., Venepally, P., Lacar, B., Bhutani, K., Linker, S.B., Pham, S., Erwin, J.A., Miller, J.A., Hodge, R., McCarthy, J.K., Kelder, M., McCorrison, J., Aevermann, B.D., Fuertes, F.D., Scheuermann, R.H., Lee, J., Lein, E.S., Schork, N., McConnell, M.J., Gage, F.H., Lasken, R.S., 2016. Using

single nuclei for RNA-seq to capture the transcriptome of postmortem neurons. Nat. Protoc. 11, 499–524. https://doi.org/10.1038/nprot.2016.015.
Krueger, F., 2012. Babraham Bioinformatics - Trim Galore! [WWW Document]. URL. https://www.bioinformatics.babraham.ac.uk/projects/trim_galore/. accessed 7.4.25.
Liberzon, A., Subramanian, A., Pinchback, R., Thorvaldsdóttir, H., Tamayo, P., Mesirov, J.P., 2011. Molecular signatures database (MSigDB) 3.0. Bioinformatics 27, 1739–1740. https://doi.org/10.1093/bioinformatics/btr260.
Liberzon, A., Birger, C., Thorvaldsdóttir, H., Ghandi, M., Mesirov, J.P., Tamayo, P., 2015. The molecular signatures database Hallmark gene set collection. Cell Syst. 1, 417–425. https://doi.org/10.1016/j.cels.2015.12.004.
López-Fortún, N., Roig-Genovés, J.V., Giménez, I., Cerdà, J., Chauvigné, F., 2025. Gonadotropins differentially regulate testicular cell adhesion and junctional complexes during flatfish spermiogenesis through the oxytocin and relaxin signaling pathways. Front. Cell Dev. Biol. 13, 1574690. https://doi.org/10.3389/fcell.2025.1574690.
López-Olmeda, J.F., Pujante, I.M., Costa, L.S., Galal-Khallaf, A., Mancera, J.M., Sánchez-Vázquez, F.J., 2016. Daily rhythms in the somatotropic axis of Senegalese sole (*Solea senegalensis*): the time of day influences the response to GH administration. Chronobiol. Int. 33, 257–267. https://doi.org/10.3109/07420528.2015.1111379.
Love, M.I., Huber, W., Anders, S., 2014. Moderated estimation of fold change and dispersion for RNA-seq data with DESeq2. Genome Biol. 15, 550. https://doi.org/10.1186/s13059-014-0550-8.
Marín-Juez, R., Viñas, J., Mechaly, A.S., Planas, J.V., Piferrer, F., 2013. Stage-specific gene expression during spermatogenesis in the Senegalese sole *Solea senegalensis*, a fish with semi-cystic type of spermatogenesis, as assessed by laser capture microdissection and absolute quantitative PCR. Gen. Comp. Endocrinol. In: 26th Conference of European Comparative Endocrinologists (CECE) 188, pp. 242–250. https://doi.org/10.1016/j.ygcen.2013.04.015.
Martin, M., 2011. Cutadapt removes adapter sequences from high-throughput sequencing reads. EMBnet.journal 17, 10–12. https://doi.org/10.14806/ej.17.1.200.
Martín, I., Carazo, I., Rasines, I., Rodríguez, C., Fernández, R., Martínez, P., Norambuena, F., Chereguini, O., Duncan, N., 2019. Reproductive performance of captive Senegalese sole, *Solea senegalensis*, according to the origin (wild or cultured) and gender. Span. J. Agric. Res. 17 (4), e0608. https://doi.org/10.5424/sjar/2019174-14953.
Martín-Robles, A.J., Aliaga-Guerrero, M., Whitmore, D., Pendón, C., Muñoz-Cueto, J.A., 2012. The circadian clock machinery during early development of Senegalese sole (*Solea senegalensis*): effects of constant light and dark conditions. Chronobiol. Int. 29, 1195–1205. https://doi.org/10.3109/07420528.2012.719963.
Milla, S., Pasquet, A., El Mohajer, L., Fontaine, P., 2021. How domestication alters fish phenotypes. Rev. Aquac. 13, 388–405. https://doi.org/10.1111/raq.12480.
Morais, S., Aragão, C., Cabrita, E., Conceição, L.E.C., Constenla, M., Costas, B., Dias, J., Duncan, N., Engrola, S., Estevez, A., Gisbert, E., Mañanós, E., Valente, L.M.P., Yúfera, M., Dinis, M.T., 2016. New developments and biological insights into the farming of *Solea senegalensis* reinforcing its aquaculture potential. Rev. Aquac. 8, 227–263. https://doi.org/10.1111/raq.12091.
Munroe, T.A., 2021. Systematic revision of the flatfish genus Peltorhamphus Günther, 1862 (Teleostei: Pleuronectiformes: Rhombosoleidae), including description of a new species from Southeastern New Zealand, with biological and ecological summaries for the species. Zootaxa 4905, 1–104. https://doi.org/10.11646/zootaxa.4905.1.1.
Murat, F., Mbengue, N., Winge, S.B., Trefzer, T., Leushkin, E., Sepp, M., Cardoso-Moreira, M., Schmidt, J., Schneider, C., Mößinger, K., Brüning, T., Lamanna, F., Belles, M.R., Conrad, C., Kondova, I., Bontrop, R., Behr, R., Khaitovich, P., Pääbo, S., Marques-Bonet, T., Grützner, F., Almstrup, K., Schierup, M.H., Kaessmann, H., 2023. The molecular evolution of spermatogenesis across mammals. Nature 613, 308–316. https://doi.org/10.1038/s41586-022-05547-7.
Ni, F.-D., Hao, S.-L., Yang, W.-X., 2019. Multiple signaling pathways in Sertoli cells: recent findings in spermatogenesis. Cell Death Dis. 10, 541. https://doi.org/10.1038/s41419-019-1782-z.
Oliveira, C.C.V., Fatsini, E., Fernández, I., Anjos, C., Chauvigné, F., Cerdà, J., Mjelle, R., Fernandes, J.M.O., Cabrita, E., 2020. Kisspeptin influences the reproductive axis and circulating levels of microRNAs in senegalese sole. Int. J. Mol. Sci. 21, 9051. https://doi.org/10.3390/ijms21239051.
Pfennig, F., Standke, A., Gutzeit, H.O., 2015. The role of Amh signaling in teleost fish -multiple functions not restricted to the gonads. Gen. Comp. Endocrinol. 223, 87–1107. https://doi.org/10.1016/j.ygcen.2015.09.025.
Print, C.G., Loveland, K.L., 2000. Germ cell suicide: new insights into apoptosis during spermatogenesis. BioEssays 22, 423–430. https://doi.org/10.1002/(SICI)1521-1878(200005)22:5<423::AID-BIES4>3.0.CO;2-0.
Qian, P., Kang, J., Liu, D., Xie, G., 2022. Single cell transcriptome sequencing of zebrafish testis revealed novel spermatogenesis marker genes and stronger Leydig-germ cell paracrine interactions. Front. Genet. 13. https://doi.org/10.3389/fgene.2022.851719.
Ramírez, D., Rodríguez, M.E., Mukiibi, R., Peñaloza, C., D'Cotta, H., Robledo, D., Rebordinos, L., 2024. Methylation profile of the testes of the flatfish *Solea senegalensis*. Aquacult. Rep. 39, 102405. https://doi.org/10.1016/j.aqrep.2024.102405.
Ramírez, D., Anaya-Romero, M., Rodríguez, M.E., Arias-Pérez, A., Mukiibi, R., D'Cotta, H., Robledo, D., Rebordinos, L., 2025. Insights into *Solea senegalensis* reproduction through gonadal tissue methylation analysis and transcriptomic integration. Biomolecules 15, 54. https://doi.org/10.3390/biom15010054.
Ramos-Júdez, S., González-López, W.Á., Huayanay Ostos, J., Cota Mamani, N., Marrero Alemán, C., Beirão, J., Duncan, N., 2021. Low sperm to egg ratio required for successful in vitro fertilization in a pair-spawning teleost, Senegalese sole (*Solea senegalensis*). R. Soc. Open Sci. 8, 201718. https://doi.org/10.1098/rsos.201718.
Riesco, M.F., Valcarce, D.G., Martínez-Vázquez, J.M., Martín, I., Calderón-García, A.A., González-Núnez, V., Robles, V., 2019. Male reproductive dysfunction in *Solea senegalensis*: new insights into an unsolved question. Reprod. Fertil. Dev. 31, 1104–1115. https://doi.org/10.1071/RD18453.
Robledo, D., Hermida, M., Rubiolo, J.A., Fernández, C., Blanco, A., Bouza, C., Martínez, P., 2017. Integrating genomic resources of flatfish (Pleuronectiformes) to boost aquaculture production. Comp. Biochem. Physiol. Part D Genomics Proteomics 21, 41–55. https://doi.org/10.1016/j.cbd.2016.12.001.
Sayers, E.W., Beck, J., Bolton, E.E., Brister, J.R., Chan, J., Connor, R., Feldgarden, M., Fine, A.M., Funk, K., Hoffman, J., Kannan, S., Kelly, C., Klimke, W., Kim, S., Lathrop, S., Marchler-Bauer, A., Murphy, T.D., O'Sullivan, C., Schmieder, E., Skripchenko, Y., Stine, A., Thibaud-Nissen, F., Wang, J., Ye, J., Zellers, E., Schneider, V.A., Pruitt, K.D., 2025a. Database resources of the National Center for Biotechnology Information in 2025. Nucleic Acids Res. 53, D20–D29. https://doi.org/10.1093/nar/gkae979.
Sayers, E.W., Beck, J., Bolton, E.E., Brister, J.R., Chan, J., Connor, R., Feldgarden, M., Fine, A.M., Funk, K., Hoffman, J., Kannan, S., Kelly, C., Klimke, W., Kim, S., Lathrop, S., Marchler-Bauer, A., Murphy, T.D., O'Sullivan, C., Schmieder, E., Skripchenko, Y., Stine, A., Thibaud-Nissen, F., Wang, J., Ye, J., Zellers, E., Schneider, V.A., Pruitt, K.D., 2025b. Database resources of the National Center for Biotechnology Information in 2025. Nucleic Acids Res. 53, D20–D29. doi:https://doi.org/10.1093/nar/gkae979.
Stuart, T., Satija, R., 2019. Integrative single-cell analysis. Nat. Rev. Genet. 20, 257–272. https://doi.org/10.1038/s41576-019-0093-7.
Tirosh, I., Izar, B., Prakadan, S.M., Wadsworth, M.H., Treacy, D., Trombetta, J.J., Rotem, A., Rodman, C., Lian, C., Murphy, G., Fallahi-Sichani, M., Dutton-Regester, K., Lin, J.-R., Cohen, O., Shah, P., Lu, D., Genshaft, A.S., Hughes, T.K., Ziegler, C.G.K., Kazer, S.W., Gaillard, A., Kolb, K.E., Villani, A.-C., Johannessen, C. M., Andreev, A.Y., Van Allen, E.M., Bertagnolli, M., Sorger, P.K., Sullivan, R.J., Flaherty, K.T., Frederick, D.T., Jané-Valbuena, J., Yoon, C.H., Rozenblatt-Rosen, O., Shalek, A.K., Regev, A., Garraway, L.A., 2016. Dissecting the multicellular ecosystem of metastatic melanoma by single-cell RNA-seq. Science 352, 189–196. https://doi.org/10.1126/science.aad0501.
Trapnell, C., Cacchiarelli, D., Grimsby, J., Pokharel, P., Li, S., Morse, M., Lennon, N.J., Livak, K.J., Mikkelsen, T.S., Rinn, J.L., 2014. The dynamics and regulators of cell fate decisions are revealed by pseudotemporal ordering of single cells. Nat. Biotechnol. 32, 381–386. https://doi.org/10.1038/nbt.2859.
Wu, T., Hu, E., Xu, S., Chen, M., Guo, P., Dai, Z., Feng, T., Zhou, L., Tang, W., Zhan, L., Fu, X., Liu, S., Bo, X., Yu, G., 2021. clusterProfiler 4.0: A universal enrichment tool for interpreting omics data. Innov. Camb. Mass 2, 100141. https://doi.org/10.1016/j.xinn.2021.100141.
Yang, Y., Zhou, Y., Wessel, G., Hu, W., Xu, D., 2024. Single-cell transcriptomes reveal spermatogonial stem cells and the dynamic heterogeneity of spermatogenesis in a seasonal breeding teleost. Development 151, dev203142. https://doi.org/10.1242/dev.203142.
Zappia, L., Oshlack, A., 2018. Clustering trees: a visualization for evaluating clusterings at multiple resolutions. GigaScience 7, giy083. https://doi.org/10.1093/gigascience/giy083.
Zhang, Z., Lin, W., He, D., Wu, Q., Cai, C., Chen, H., Shang, Y., Zhang, X., 2023. Aquaculture environment changes fish behavioral adaptability directly or indirectly through personality traits: a case study. Rev. Fish Biol. Fish. 33, 1423–1441. https://doi.org/10.1007/s11160-023-09779-2.
Zheng, G.X.Y., Terry, J.M., Belgrader, P., Ryvkin, P., Bent, Z.W., Wilson, R., Ziraldo, S.B., Wheeler, T.D., McDermott, G.P., Zhu, J., Gregory, M.T., Shuga, J., Montesclaros, L., Underwood, J.G., Masquelier, D.A., Nishimura, S.Y., Schnall-Levin, M., Wyatt, P.W., Hindson, C.M., Bharadwaj, R., Wong, A., Ness, K.D., Beppu, L.W., Deeg, H.J., McFarland, C., Loeb, K.R., Valente, W.J., Ericson, N.G., Stevens, E.A., Radich, J.P., Mikkelsen, T.S., Hindson, B.J., Bielas, J.H., 2017. Massively parallel digital transcriptional profiling of single cells. Nat. Commun. 8, 14049. https://doi.org/10.1038/ncomms14049.